

Landslides (2018) 15:1233–1251
 DOI 10.1007/s10346-018-0973-5
 Received: 4 December 2017
 Accepted: 26 February 2018
 Published online: 13 March 2018
 © Springer-Verlag GmbH Germany,
 part of Springer Nature 2018

Martin Bednarik · René Putiška · Ivan Dostál · Rudolf Tornyai · Karel Šilhán · Filip Holzer · Karol Weis · Ivan Ružek

Multidisciplinary research of landslide at UNESCO site of Lower Hodruša mining water reservoir

Abstract This article presents a multidisciplinary approach to the assessment of slope deformation at the Lower Hodruša mining water reservoir, which is part of a UNESCO cultural heritage site. The multidisciplinary approach was used to develop remedial measures. The Lower Hodruša mining water reservoir is situated in the Hodruša-Hámre municipality near Banská Štiavnica in the central part of Slovakia. The first mention of the construction of the reservoir is from 1743, and according to historical records, there were problems with slope stability already at that time. Nowadays, to increase the volume of water available for technical operations in the Hodruša valley, the decision was made to increase the dam's output capacity. Slope movements were first detected while the reservoir was being drained. A part of the left shore 50 to 150 m from the dam crest moved, damaging adjacent buildings. The Hodruša-Hámre municipal authorities declared an emergency on 24 August 2015 because of the appearance of cracks in the asphalt surface of the national road and its subsidence. The main discontinuity conformed approximately to the contours of the known landslide area on the south side of the reservoir. The significant deformations involving the 0.20-m subsidence of the service road were reported during heavy rainfall in October 2014. A range of geoscientific disciplines was used to develop a detailed description of the landslide area and to determine the cause of the slope deformation. The depth and course of the shear surface were measured using boreholes and geophysical methods; the historic development of the landslide was analysed using dendrochronological measurements; and the present horizontal and vertical movement of the landslide over one and half years was determined using geodetic monitoring based on a network of stabilised points and inclinometer measurements.

Keywords Banská Štiavnica · Landslide · Lower Hodruša mining water reservoir

Introduction

Banská Štiavnica and its surroundings are amongst the most beautiful and historically most significant places in Slovakia. It is probably the oldest mining town in Europe, and its ore deposits have been exploited since the Bronze Age. The wealth from centuries of mining has resulted in a rich architecture of palaces, churches and squares; and Banská Štiavnica was a European centre of mining education from the late sixteenth century. Because of its exceptional value, the historic town of Banská Štiavnica and the technical monuments in its vicinity including artificial mining water reservoirs (operating in the area since the sixteenth century, first in 1510) were listed by the United Nations Educational, Scientific and Cultural Organization (UNESCO) as a World Heritage Site on 11 December 1993.

The dam body of this water reservoir has been refurbished and upgraded several times in history, for example, in the years 1786, 1812, 1823, 1960 and 2008. However, the water reservoir was located

directly adjacent to the south-facing, relatively stabilised landslide (Pleistocene in age), with an area of about 50 ha, denudated by erosion and less stable younger intrusions of weathered quartz-diorite porphyry in a contact metamorphosed lava flows of pyroxene andesite. At the time of the general reconstruction of the discharge facility in the years 2013–2015, part of this sliding body was reactivated at a low water level in the reservoir and after heavy rainfall.

In May 2013, Slovak Water Management Enterprise, state enterprise, Banská Bystrica, began the reconstruction of the sluiceway of the Lower Hodruša mining water reservoir. The planned reconstruction of the reservoir sluiceway required the discharge of all water stored in the reservoir. Reconstruction began on 29 July 2013 with the slow discharge of the reservoir began according to a schedule covering over 3 months from 29 July 2013 (elevation 528.08 m a.s.l.) to 14 October 2013 (elevation 514.00 m a.s.l.). The time for discharge in 2013 was reduced, because the level was already low after below average precipitation combined with the need to maintain a minimum maintenance flow in the Hodrušianka Stream to supply a breeding ground for sport fishing and technological water for an ore treatment plant. All fish and other aquatic fauna, including protected species, were removed from the reservoir for their protection in the period 12–13 October and 19–20 October 2013.

The approved operating rules of the reservoir allowed the reservoir's level to be lowered by 0.50 m per day, but owing to its low output capacity, the actual decrease in the level of the reservoir was only 0.25 to 0.30 m per day. Discharging water from the water reservoir naturally caused release of the tension stabilising the foot of the sliding slope. The first slope movements were detected in spring 2014. A part of the left shore 50 to 150 m from the dam crest began to slide, causing damage to adjacent buildings. Significant deformations involving the 0.20-m subsidence of the service road were reported during heavy rainfall in October 2014.

Besides heavy rain, one of the main causes of the landslide activation was the uneven pore pressure release. The problem was that during discharge the level of the mining water reservoir went down faster than the groundwater level in the slope, which caused the pore pressure to increase. After the completion of the controlled discharge, the reservoir area was episodically flooded by occasional rainfall in the micro drainage basin. The torrential rains in the spring and summer of 2015 probably caused the saturation of the surrounding environment including the exposed rock mass in the reservoir area.

The refilling of the reservoir began at the end of May 2016, while in March 2016, the water level was 4 m below the minimum operating level (518.0 m a.s.l.). Initial filling of the reservoir complied with the maximum daily rise in the level of 3 cm, later just 2 cm. The water level has been continuously monitored since August 2014 using a network of observation probes.

In critical cases, a change in the use of an artificial reservoir from its original purpose to a new economic model can lead to an increase in surface flow that triggers erosion and relief changes in the micro drainage basin and in the bed of the reservoir. Many of these negative trends are also associated with a change in the owner or administrator of a reservoir. Several recent studies have investigated the changes in total storage capacity and silting of reservoirs around Banská Štiavnica in recent years (Kubinský et al. 2014a; Weis and Kubinský 2014; Fuska et al. 2017). The problems of environmentally degraded mining areas in Slovakia are currently described, for example, in Čech and Krokusová (2017). All the aforementioned factors often occur in river basins together with negative changes in the secondary landscape structure that lead not only to increased sediment in the reservoirs and changes in their biological equilibrium and water quality but also gradually to their complete silting up and extinction. The Altınapa Reservoir in Turkey lost 33.4% of its storage capacity between 1967 and 2009 (Ceylan et al. 2011). The capacity of Lake Mladotice in Czechia, which was created by a landslide, decreased by 26.5% in the period from 1972 to 2003 (Janský et al. 2010). The unfavourable condition of lakes and reservoirs affected by sedimentation has also been described in neighbouring Poland, where a total of 25 lakes lost 9.9% of their accumulation capacity over 50 years (Choiński and Ptak 2009). If a drainage basin is deforested or inappropriately managed or used, any areas that are prone to landslides or slope deformation will be easily activated by episodes of torrential rain. Sedimentation dynamics in incompact rocks in connection with the creation of landslide-dammed lakes has been studied by foreign authors such as Smolková et al. (2009).

As known from several cases in the world, minor landslide reactivations with hardly visible surface deformations often precede a large landslide event (Petley and Allison 1997; Pánek et al. 2011). Thus, the question is if some minor prelandslide reactivation events in the case of the Hodruša landslide occurred as well. Such

data can be important for potential triggers analysis or as a basis for early warning systems (Floris and Bozzano 2008). As systematic landslide monitoring has been carried out only since 2014, the knowledge about possible events before this date does not exist. However, tree ring-based (dendrogeomorphic) approaches are currently thought to be the most precise method for past landslide events dating if the landslide is covered by trees (Alestalo 1971). The approach is based on the ability of trees to respond in their growth to landslide events that affected their roots, stems or branches (Lopez-Saez et al. 2012; Stoffel et al. 2013; Šilhán 2017). According to Migoń et al. (2014), trees are able to record in their tree ring series landslide events even in the range of several millimetres. Thus, the use of such methods for uncovering past landslide events in the unmonitored or remote inhabited areas is highly valuable and recommended.

Geographical, geological and technical settings

Geographical settings

The territory of interest is located in the central part of Slovakia in Banská Štiavnica district in the central part of the central part of the Štiavnica Mountains (Fig. 1). The Štiavnica Mountains have an area of 872 km². The altitude ranges from 195 m above sea level at the surface of the River Hron at the Slovak Gate to 1009 m above sea level at the summit of peak Sitno. In orographic terms, the Štiavnica Mountains are part of the central Slovak volcanic complex, the largest volcanic mountain range in Slovakia.

The current relief is quite different from the original volcanic relief. The period produced a smoothly modelled relief—a highland plateau—traces of which can be found in the Štiavnica Mountains to this day. A noticeable morphological feature is frequent pronounced lava flows with rock forms that contrast with the smoothly modelled relief on pyroclastic rocks. The diverse assortment of volcanic rocks with varying levels of resistance



Fig. 1 Location map of the Lower Hodruša mining water reservoir

combined with varied erosion and denudation processes in the Štiavnica Mountains have resulted in a varied relief with strong horizontal divisions, in which branching mountain ridges alternate with furrows and deeper and shallower valleys.

According to the climatic classification for Slovakia (*Landscape Atlas of the Slovak Republic 2002*), the territory under consideration is a moderately warm M region, subtype M6, which means a moderately warm, damp upland region. The average annual air temperature is 6 to 8 °C; total annual precipitation is on average 700 to 800 mm, and the area has on average 80 to 100 days of snow coverage.

A unique feature of the Štiavnica Mountains that is of significance on the European level is the water management system developed over several centuries to support mining operations. The system is made up of collection and transport ditches, drainage tunnels and artificial water reservoirs—the *tajchy*. Out of a total of 60 artificial reservoirs that were constructed, 50 were used for mining activities. This water management system is now an important cultural and technical heritage monument. More than 20 water reservoirs have been preserved in the area. They now serve aesthetic and recreational functions and only the Rozgrund *tajch* is used to supply drinking water.

Geological settings

The wider environment around the mining water reservoir is built by quartz-diorite porphyry belonging to the second phase in the development of the Štiavnica stratovolcano (Studená formation, Banisko intrusive complex). The rock is characterised by high strength under a pressure of 50 to 100 MPa, in places with very high strengths of 100 to 250 MPa. The deformation modulus E_{def}

varies between 1500 and 6000 MPa (according to crack density) and the Poisson number varies between 0.15 and 0.25. Coarse quartz-diorite porphyry of the Hodruša type is found in the studied area in larger quantities on the right shore of the Lower Hodruša mining water reservoir and to a lesser extent also on the left shore (Fig. 2). It is a sill-type body that intruded at the interface between the bedrock and the lower volcanic structure. The eastern edge of the body, which has been strongly divided by graben and horst tectonics and denudation, begins in the Kohútska Valley and continues north to the slopes of Komenská Hodruška. In the Banská Hodruša area, traces of the lower volcanic structure are preserved in the bed under the sill. The intrusion re-emerges at the surface from under the lower volcanic structure together with the underlying granodiorite in a partial horst south-east of the Lower Hodruša mining water reservoir. The body of quartz-diorite porphyry has a relatively uniform composition. The rock is massive with a grey-green shade (propylitization) with block and columnar jointing. It has a coarse porphyry texture. The main components are potassium feldspar and quartz. Plagioclase and dark minerals are also present. It has undergone some hydrothermal transformation in which plagioclase is replaced by sericites and carbonates. The dark minerals have undergone intensive transformation resulting in their replacement by chlorite, calcite and quartz (Konečný et al. 1998).

Direct contact with the pre-Quaternary base results in the creation of eluvial sediments from the weathering of the original parent rock. Besides a degree of weathering, the rocks are affected by hydrothermal transformation (propylitization, argillization) and tectonic disruption. The eluvial sediments form a more pronounced cover particularly in areas of flat peaks, and they are

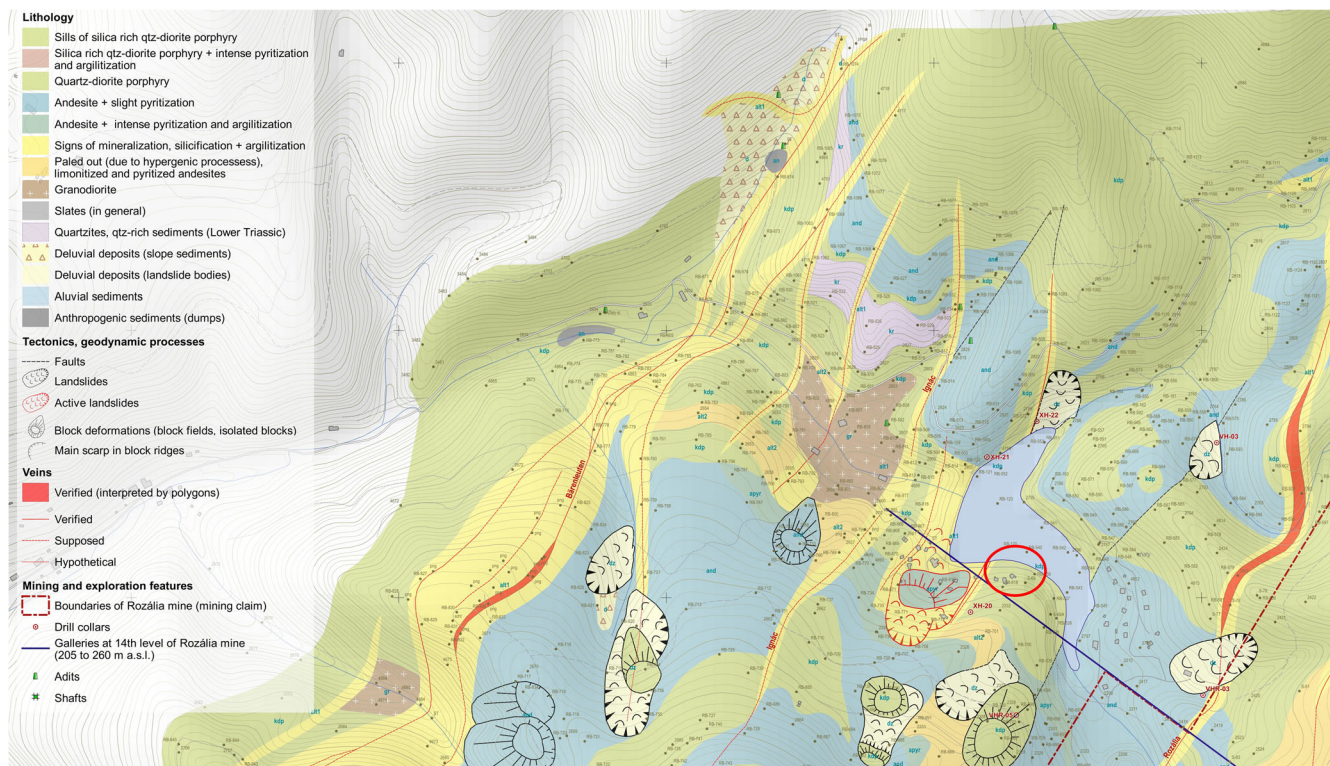


Fig. 2 Geological map of the environs of the Rozália Mine (Hodruša-Hámre) (Lexa 2016)

mainly covered by slope sediments. The eluvial and slope sediments originated on the slopes of the mountain ridges, particularly at sites where weathering, erosion and denudation during the Neogene and Quaternary periods caused long-term disturbances in the rock bed, especially following uneven tectonic disturbances. The slope sediments cover the adjacent slopes; they have different grain composition, comprising mainly slope sediments, silt containing sandy admixture and parent rock debris of various sizes. Larger thicknesses form at the foot of the slopes, where the relief is less steep. In some places, a clay-stone scree forms containing predominantly weathered volcanic rocks. In the deep Hodruša Valley, the Hodruša Stream has deposited fluvial sediments with smaller grain sizes. Because of the morphology of the terrain, the steep slopes and the valleys, the fluvial sediments have boulder or large boulder grain size, and at the higher levels in the valley, there is very little gravel or sand-sized sediment. Gravel and sand sedimentation is more characteristic of the lower and less steep parts of the valley (essentially between the Banská Hodruša and the Hron valley). In the lowest parts of the valley, it is common to find silt admixtures in fluvial sediments; fluvial accumulations are covered by fine-grained fluvial deposits.

There has been mining in the Banská Štiavnica region since the middle ages. Intensive activity has produced countless spoil heaps of various sizes and thicknesses, which can be up to tens of metres in places. Most of them are old spoil heaps, and they now tend to be covered by vegetation if they were not produced by recent mining activity.

The complex geological-tectonic structure, climatic-hydrological conditions, weathering, etc. create conditions for the release of massifs, the emergence of slope movements in the form of block movements, landslides, earth flows, rock falls, which lead to changes in the relief. The strong contrasts in the relief of the territory also promote erosive and accumulative geodynamic phenomena. In the mining water reservoirs or *tajchy*, there is abrasion of the shores. Landslides are frequent, especially in areas with intensive hydrothermal changes, where argillized zones form, as can be seen on the slopes above the Lower and Upper Hodruša fish ponds. Another factor that favours landslides is the presence of volcanoclastic rocks such as tuffs and pumice tuffs in the bed of the lava bodies (Konečný et al. 1998).

Construction and reconstruction phases of Lower Hodruša mining water reservoir

The Lower Hodruša mining water reservoir was created by damming the valley of the Hodruša Stream with a 199-m-long dam at an altitude of 528 m a.s.l. The dam is 22 m high with a maximum crest width of 5.70 m. The reservoir has a water capacity of 641,000 m³ and covers an area of 4.33 ha. The reservoir's maximum depth is 21 m. In 1992, the Lower Hodruša mining water reservoir was inscribed in the UNESCO World Heritage List as part of the site Banská Štiavnica and its surroundings.

One channel from the outlet carried water 500 m to power ore-crushing equipment at Rabenstein and then continued another 1000 m to the Lill mineshaft. Another channel ran to the Zipser mineshaft and then to the ore crusher at the Upper Hodruša Mining Works via Barenleuten with a length of around 1500 m. Water was diverted from the Hodruša Stream below the dam to foundries, mines and crushing plants via many channels with a total length of several tens of kilometres.

The dam is a heterogeneous earth-fill dam constructed from five sections: the sealing core is made of compacted clay and silt; the air and water sides are an earth mound; the water side is reinforced with stones and a stone wall supports the air side slope at its foot.

The mining water reservoir was built between 1743 and 1744 under the supervision of Samuel Mikoviny, the head of Mining Academy in Banská Štiavnica till 1748, at the meeting place of two valleys under the peaks Tanáda and Paradajz at the head of the Hodruša Valley. The valley of the Hodruša Stream was blocked by an earth-filled dam. In July 1744, the dam reached a height of 14 m but there were insufficient funds to continue work and it did not reach its planned design height of 20 m. The dam was raised by another 9 m in 1786. In 1812, several cracks were found on the air side of the dam. In 1815, the sunken middle part of the dam was filled in and fresh clay was pounded down on it to level it with its surroundings. To prevent the increasingly frequent subsidence of the air side of the dam, two spiked oak posts, two fathoms long (around 4 m), were installed into the dam. Repair work commenced again in 1823 including beating earth into places where extensive subsidence had taken place and raising the stone supporting wall at the foot of the dam by 6 ft. Further work was carried out in stages: raising the embankment, building a drainage (bypass) tunnel, repairing the sluiceway, etc. (Kašiarová 2003). Figure 3 shows the location of prospecting fields at the end of the eighteenth century.

In 1960, a flood broke the safety overflow and sluiceway and a general overhaul was commenced the same year. Work was completed in 1966. The dam was partially raised and reinforced in the middle part also in the year 2008. The most recent overhaul of the dam, sluiceway and water tunnel was conducted from 2013 to 2016. The bottom outlet is at 514 m above sea level. The minimum and maximum operating levels of the reservoir are 518 and 528 m above sea level. The overflow sill is at an altitude of 528.63 m above sea level.

Active slope deformation and analyses of triggering factors

The actual slope deformation can be characterised as an active earth slide in the foreground of a fossil stabilised slope deformation, probably dating from the Pleistocene. The landslide is 92 m long and 70 m wide (Fig. 4f, h). The total area of the landslide is 5007 m². The landslide was measured using a GNSS Trimble R4 with a subcentimetre accuracy on 22 November 2014.

In the separation zone of the landslide, there are three recreational chalets; the transportation part is deforming a road—the only connection linking Hodruša-Hámre to the working Rozália gold mine and the Salamander SKI resort. The accumulation part of the landslide is in the discharged reservoir ending just above the waterline. Field survey identified a number of oak wood posts several tens of centimetres in diameter in the foot of the landslide (Fig. 4g). They had probably been used to control the landslide in previous centuries, perhaps immediately after construction and during the filling of the reservoir.

The recreational chalets are currently affected by varying degrees of structural damage in the form of hairline and open cracks in the external walls (Fig. 4b, e). The access road has subsided by 20 cm, and the accumulation is marked with cracks in three levels with a width of up to 10 cm—end of February 2014—cracks with a width of 0.5–1 cm, regular monitoring of crack development; in following months, they were observed to

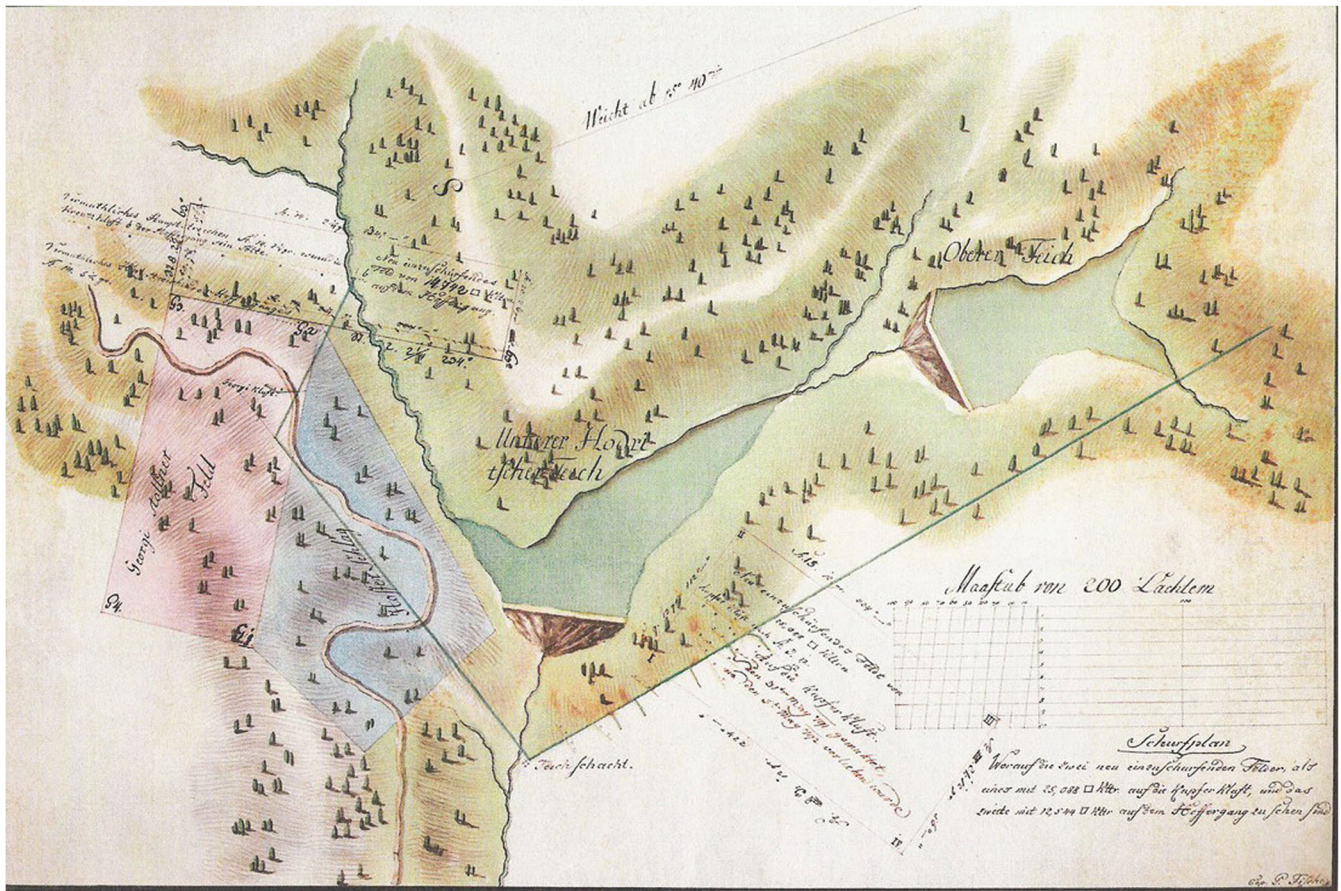


Fig. 3 The Upper and Lower Hodruša reservoirs on a map of new prospecting fields in the 1790s (copy by P. Fischer) (source: www.slovenskiwynalezcovia.webz.cz/tajchy.htm)

widen and appear also inside the chalets; 13 May 2014—the cracks are up to 3 cm wide; September to October 2014—largest movement recorded—opening of cracks in tens of centimetres (Fig. 4c); further movement was observed after survey work on 14 November 2014—widening by around 1 cm.

Technical work and geophysical measurements realised in December 2014 detected the shear plane at a depth of 4.8 m at borehole BH-2 and 5.9 m in the vicinity of borehole BH-1 (Fig. 4d). It is represented by grey clay with a soft to very soft consistency that is highly plastic, sticky and contains 15% rough fragments. The fossil basal shear plane is at the border of the Quaternary sediments and Middle Miocene rocks represented by pyroxene andesite and quartz porphyry.

One causal factor in the slope movement was uneven pore pressure release from the slope, because during discharge, the level of the mining water reservoir went down faster than the reduction in pore pressure in the slope; another factor was the intensive rain in August and September 2014.

All epochs of landslide reactivation or increases in the size of cracks in the slope above the reservoir can always be dated to the week following at least three previous weeks with a sum total precipitation greater than 30 mm/week. Another case is reactivation caused by a single week with summary rainfall exceeding 60 mm/week. As an analysis of precipitation data showed, the events of 2013 were a combination of both conditions. Another

necessary factor was the decrease in the water level in the reservoir, which reduced the pressure against the direction of the slide (hydrostatic pressure from the water column).

This dependency was confirmed for nearly all the events observed in recent decades. An example is the situation in 1974 to 1976, when the water level in the reservoir fell as a result of low precipitation in the previous year and the relatively dry winter in 1974/1975 combined with the need to maintain a constant supply of water to downstream consumers. There was heavier precipitation in March and April 1975, but there was alternation of dry and wet weeks. The catastrophic flood on 24 June 1975 was preceded by nearly 6 weeks with aggregate precipitation over 20 mm/week and 5 weeks with aggregate precipitation of 30 mm/week. A very similar situation was repeated in 1977 (Vonšáková 2017). This results in the statistical processing of rainfall sums, with minimal time delays, correspond to data obtained from dendrochronological research. Once again, years 1975 and 1977 are clearly significant.

The situation in 2014–2016 was very similar (Fig. 5). This also saw a combination of a relatively dry year followed by a heavy precipitation combined with a long-term fall in the water level caused by the reservoir's gradual emptying for reconstruction of the dam. The distribution of precipitation in the first years of the described series is diametrically different from that in the subsequent years, when there were incidents of days or weeks with



Fig. 4 Photodocumentation on active slope deformation. **a** General overview of Lower Hodruša mining water reservoir taken from the dam. **b** Detail photo of open cracks on one of the chalets situated in main scarp area. **c** Open cracks in accumulation part of the active landslide. **d** Material of shear plane. **e** Open cracks inside of chalet. **f** Photo of active slope deformation taken from the dam. **g** Old remediation works from the eighteenth century—oak wood posts. **h** Situation map of landslide with realised boreholes and geophysical measurements profiles

high precipitation, but such periods were not gathered together and were separated by dry periods. The effect of the discharge rate cannot be determined, and only high aggregate precipitation combined with low levels has been confirmed as determinant factors.

A comprehensive table (Table 1) shows history, events affecting slope stability and investigations done at concrete time.

Methods and materials

Geophysical work

Electrical resistivity tomography (ERT) is a geoelectrical method widely applied to obtain 2D and 3D high-resolution images of the resistivity subsurface patterns in areas of complex geology (Griffiths and Barker 1993). The general principle for electrical

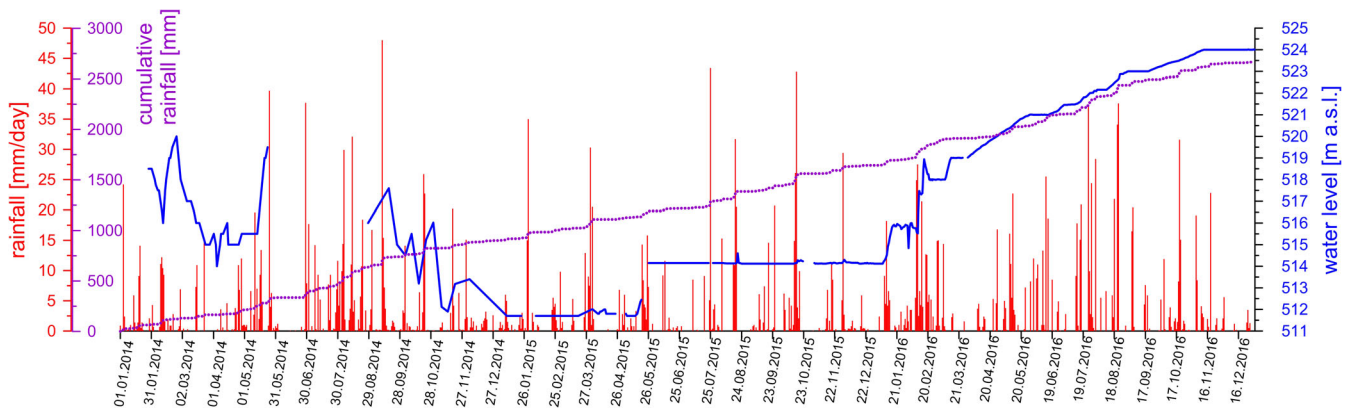


Fig. 5 Total rainfall in millimetres/day and the water level in the reservoir from the year 2014 to 2016

surface resistivity measurements is to use a string of evenly spaced electrodes pushed into the ground surface along a measuring line. Overview descriptions of electrical surface resistivity surveying techniques are given by Dahlin (2001) and Auken et al. (2006), for example.

The ERT method was applied in order to depict the geometric features of the landslide and estimate the thickness of the material mobilised, as well as to determine the course of the shear surface.

Geophysical measurements were made on two profiles. Profile ERT-H1 followed the direction of movement of the slope deformation from the separation zone through the transportation zone to the toe of the landslide (Fig. 6) over a distance of 94 m with 2 m between electrodes. Profile ERT-H2 was laid out at right angles to profile ERT-H1 in the reservoir area. It is 117 m with electrodes at 3-m intervals.

The dipole–dipole array configuration was chosen for its depth of penetration and good resolution in identifying lateral

Table 1 Comprehensive table of main landslide events

Date—year	Event	Investigations
1743–1744	Construction of the reservoir.	Slope stability problems occurred; oak wood posts installed in the foot of deformation.
1786, 1812, 1823, 1960, 2008	Refurbishing and upgrading of the dam part.	No movements/no records.
1975, 1977	Movements detected by dendrochronological research done within this study. Movements were activated due to low water level in reservoir, dry period, increased water supply to consumers, together with heavy rainfalls.	No investigations.
2013	General reconstruction of the discharge facility began by controlled discharging water from the water reservoir (0.20 to 0.30 m per day).	No movements.
Spring 2014	First slope movements were detected. A part of the left shore 50 to 150 m from the dam crest began to slide, causing damage to adjacent buildings.	First stakeholder meetings, increased need to monitor the situation.
August and October 2014	Heavy rainfalls, significant deformation of the road up to 0.20 m, cracks in tens of centimetres occurred on adjacent buildings.	Project of engineering geological survey.
December 2014	Realisation of engineering geological survey.	BH-1, BH-2 boreholes realised within landslide body, laboratory testing, geophysical measurements, stability calculations, dendrogeomorphic research.
April 2015	Geodetic monitoring.	Geodetic observation points installed.
24 August 2015	Significant deformations of the road and on the buildings continues.	State of emergency declared by Hodruša-Hámre municipality.
September 2015	Engineering geological survey, geodetic network monitoring.	Inclinometric boreholes and piezometric borehole were installed.
October–November 2015	Remediation works.	Anchored pile concrete wall realised, nine gypsum targets installed on buildings.
Nowadays	Slow controlled filling of the water reservoir.	Monitoring.

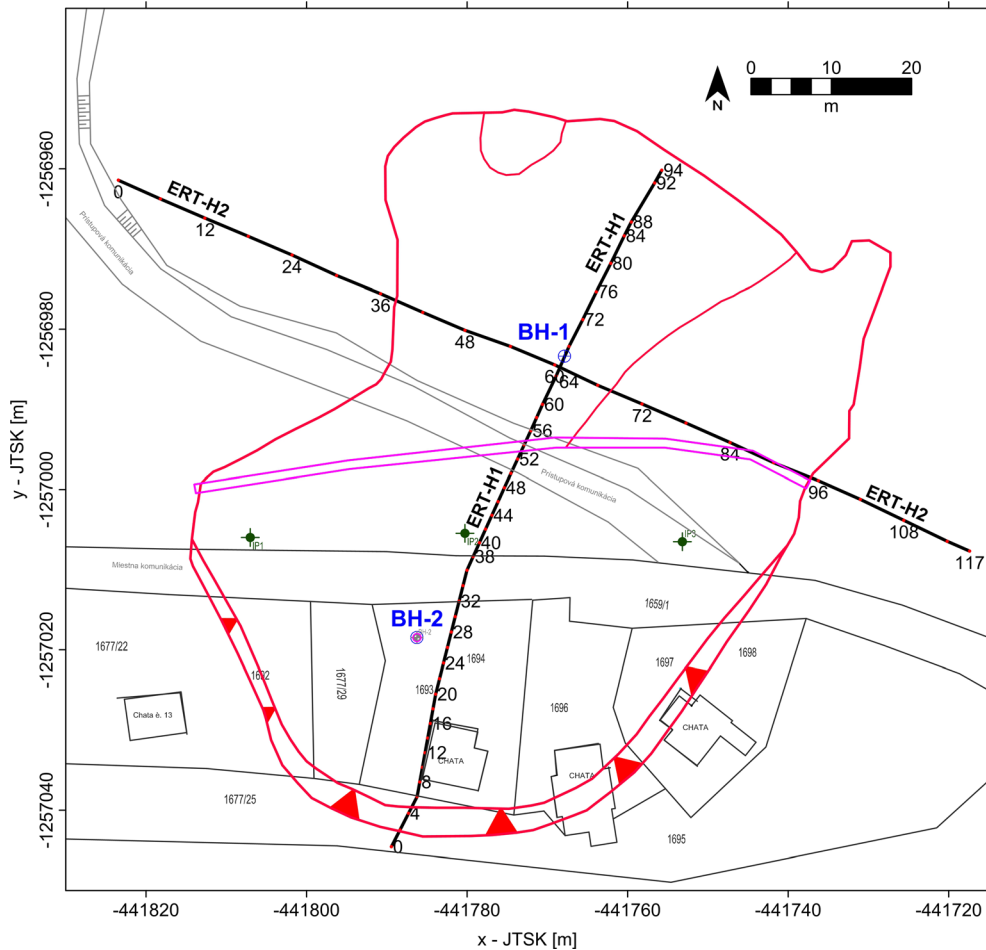


Fig. 6 Locations of geophysical profiles

heterogeneities. To maintain a higher signal-to-noise ratio, separation constants with values from one to four were used (Dahlin and Zhou 2004).

A finite element forward modelling routine was used to compare the measured values with those that theoretically could be obtained for a model of the ground, and the resistivity distribution of the model was adjusted iteratively to obtain the best fit to the measured values. In this case, the RES2DINV program was used to carry out smooth (L2-norm) inversion (Loke et al. 2003).

The results of the inversion calculation produced an inverse resistivity model that was compared with information on the lithology and shear surfaces from the drilling work in boreholes BH-1 and BH-2.

Geophysical measurements and their interpretation are an ideal basis for resolving stability questions, because they define the relief of the area and extend the point-based information from boreholes to a line, an interpreted engineering-geology profile.

Dendrochronology

The identification and dating of potentially older landslide events was realised using dendrogeomorphic (tree ring based) methods. Trees with visible potential signs of past landslide activity

(particularly tilted stems) were selected for the sampling and their position was recorded using a Trimble R8 GNSS device. Trees were sampled in the upper part of the landslide reactivated in 2014 and on the relatively stable slope located above this fresh landslide. All selected trees were sampled using Pressler increment borer (maximal length 40 cm; diameter 0.5 cm). Four increment cores were extracted from each tree in four directions (each perpendicular to the previous) in the height of maximal stem bending. Samples were processed following the standard approach (e.g. Stoffel and Bollschweiler 2008) including samples drying, gluing into wood supports, sanding with the gradual row of sand papers, tree ring counting and rings widths measurement using TimeTable (0.01-mm accuracy) and PAST4 software (VIAS 2005). Increment curves from trees without any visible growth disturbance were used as a reference chronology for cross-dating with increment curves from disturbed trees to correct possible false or missing rings. Growth disturbances (GD) possibly induced by past landslide movements were identified in the next step. Reaction wood as a response to stem tilting and abrupt growth suppression as a response to damage of root system by subsurface movements were used as a signal in tree ring series. GD were considered as landslide induced only if they did not occur in the reference chronology simultaneously. The GD chronology was expressed

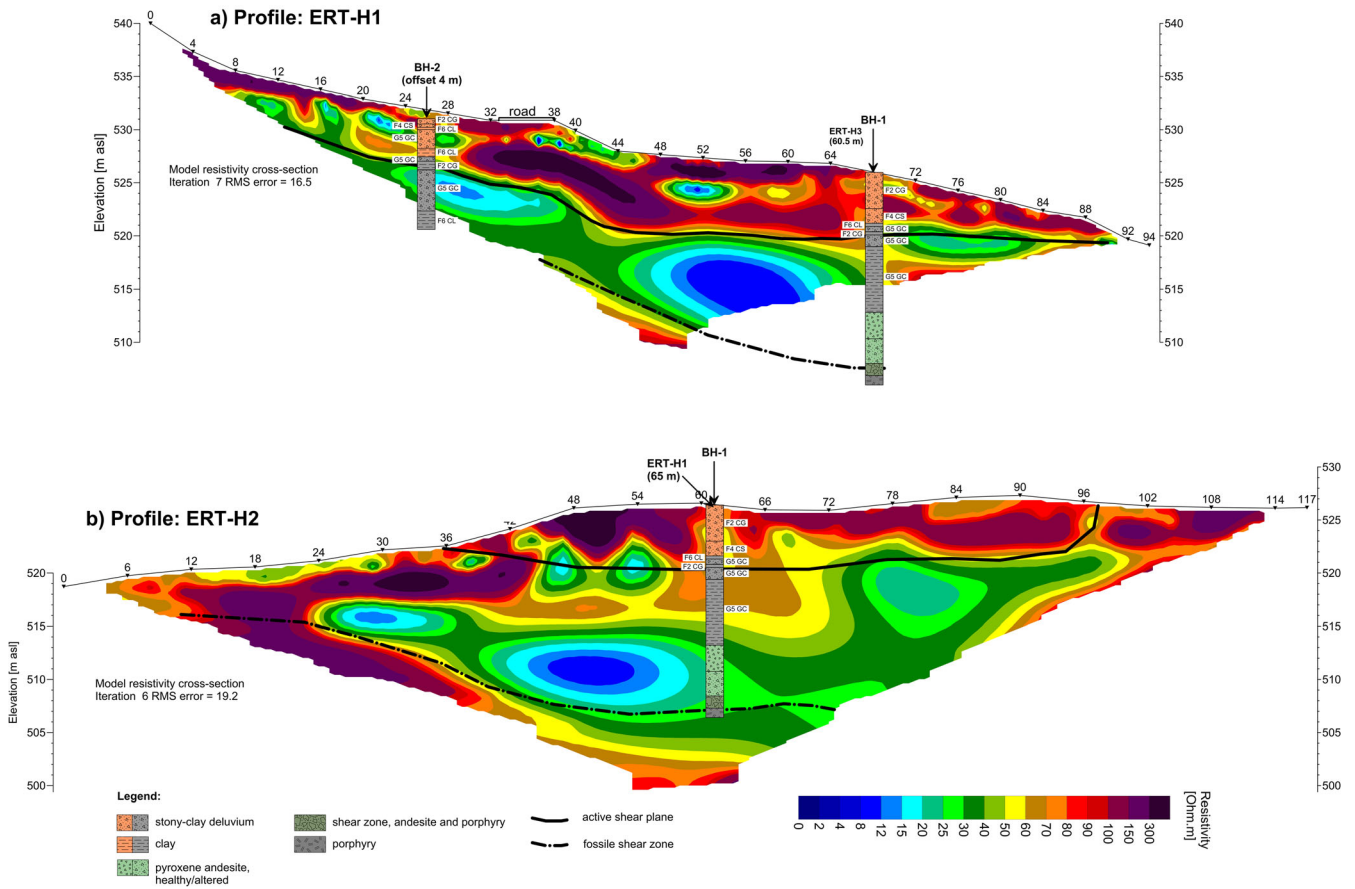


Fig. 7 ERT results. **a** Inverse resistivity cross-section of profile H1. **b** Inverse resistivity cross-section of profile H2, with lithological information from the drilling works and interpreted active/fossil shear plane

in the form of event-response (I_t) index defined according to Shroder (1978) as

$$I_t = \frac{\sum R_t}{\sum N_t} \times 100\% \quad (1)$$

where R_t is the number of tree with GD in year t , and N_t is the number of all living trees in year t . Considering the total number of sampled trees, the minimal value of the I_t index for landslide event determination was selected 5% and at least two trees had to contain GD simultaneously (Corona et al. 2014). The recurrence interval of GD was calculated for each tree when the tree age was

divided by the number of recorded GDs. The point values of recurrence intervals were spatially interpolated for reconstruction of past spatial distribution of movement events.

Inclinometric measurements

Inclinometer measurements were taken using a Geokon inclinometer probe with a measurement interval of 0.5 m. The full equipment consisted of the probe itself, a 50-m cable wound on a reel equipped with a Bluetooth interface that communicates with a portable handheld computer. The inclinometer system comprised the inclinometer casings, the probe, the control cable and a reader unit. The PVC inclinometer casings (diameter 67 mm) have longitudinal grooves in two perpendicular directions to ensure the

Table 2 Sampled trees and dated growth disturbances

	Actual active landslide	Old landslide	Total
Sampled trees	23	16	39
Samples (increment cores)	92	32	124
Reaction wood	23	8	31
Abrupt growth suppression	19	9	28
All growth disturbances	42	17	59

Table 3 Dated events and their frequency

	Actual active landslide	Old landslide
Five trees since	1934	1933
Dated events	6	3
Mean recurrence interval (years)	13.7	27.7
Mean decadal frequency	0.7	0.4

probe remains oriented in the predetermined direction. They are installed directly at a near vertical angle in a construction element or borehole (the space between the casing and the wall of the borehole and the borehole wall is filled with a bentonite-cement mixture). The grooves of the guide casings should preferably be oriented in the expected direction of movement.

Technical parameters: measuring base 500 mm, measuring range $\pm 53^\circ$, resolution 0.02 to 500 mm, working temperature -20 to 50°C (www.geoexperts.sk).

Geodetic measurements

The primary objective of geodetic monitoring was to measure the dynamics (velocity) and the direction of movement of the individual parts of the slope in the reactivated landslide during the reconstruction works in the floodplain area. Considering the observed dynamics of the landslide, whose first effects were hairline cracks in the asphalt paving and then the subsidence of a part of the national road, it was proposed that monitoring should be implemented over a wider part of the landslide area including the exposed dry part of the reservoir shore in front of the landslide. In the first phase, a total of 121 geodetic points were installed, just under half of which were situated above the level of the national road with one line following the asphalt roadway. The remaining larger group of points was installed in the reservoir area below the usual shoreline. The monitored points were laid out in a regular $10 \times 10\text{-m}$ grid. The method for field measurement and data set processing is based on the work of Kasza (2016) and Kubinský et al. (2014b).

All the installed points were stabilised with 35 and 40 cm TRNIK geodetic anchors and signalised with Geoharpon $10 \times 10\text{-cm}$ red plastic heads. On the asphalt roadway, the points were stabilised using 5-cm GEOCKE coloured geodetic pins and signalised with a 40-mm diameter pad. Regular measurement of

the monitored points and reference pins in the basic monitoring network of the renovation contractor and the reservoir administrator Slovak Water Management Enterprise, state enterprise, Banská Bystrica was conducted using the GNSS receiver ALTUS APS3 with a Handheld Nautiz X7 control unit using the Carlson SurvCE software application. High accuracy of real-time measurements was achieved by using the GSM network and the SK-POS RTK (real-time kinematic) service. For orientation in unfamiliar terrain, cartographic data was visualised and superimposed using an ALGIZ 7 field work tablet and an ALGIZ XRW notebook from Handheld.

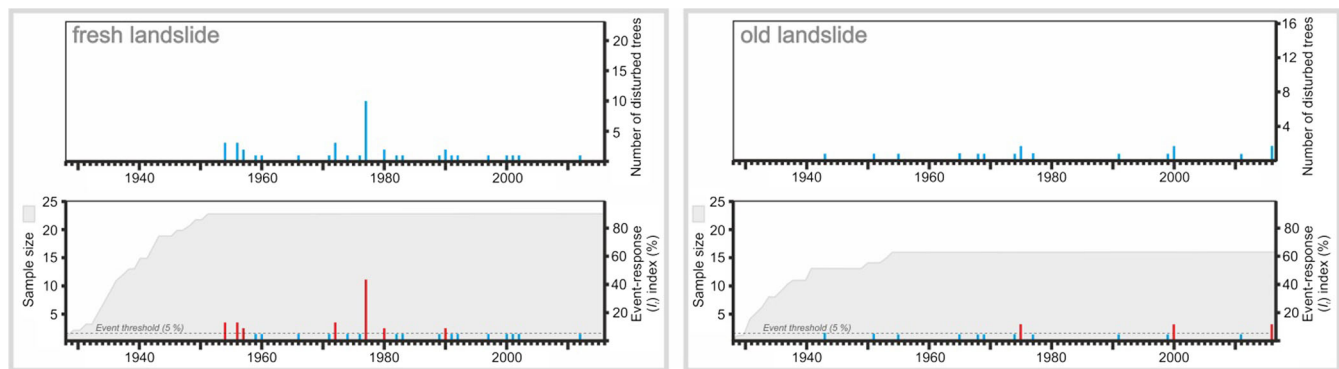
Gypsum targets

Before the remedial work on the landslide, nine gypsum targets were installed on the three damaged chalets in the deformation area on 30 October 2015 to detect signs of further deformation over 3 months. Five targets identified as G-1 to G5 were applied to the damaged chalet. Two targets were applied to the damaged chalet to the right of previous one and labelled PG-1 and PG-2, and two were applied to the damaged chalet to the left and labelled LG-1 and LG-2.

Stability assessment

The results of the technical works, the geophysical measurements and laboratory tests were used to construct an engineering-geological model of the landslide. The engineering-geological model was transformed into a mathematical slope model.

Stability calculations were done using geotechnical software GEO 5 (Fine Ltd.), modulus Slope Stability. It enables design and analysis of slope stability with circular or polygonal surface and automatic optimization of slip surface. It cooperates with all programs for analysis of Excavation Designs and Retaining Wall Designs. It allows the insertion of anchors, georeinforcements, additional loads and earthquake effects to calculations.

**Fig. 8** The chronology of landslide events expressed as an event-response (I_t) index

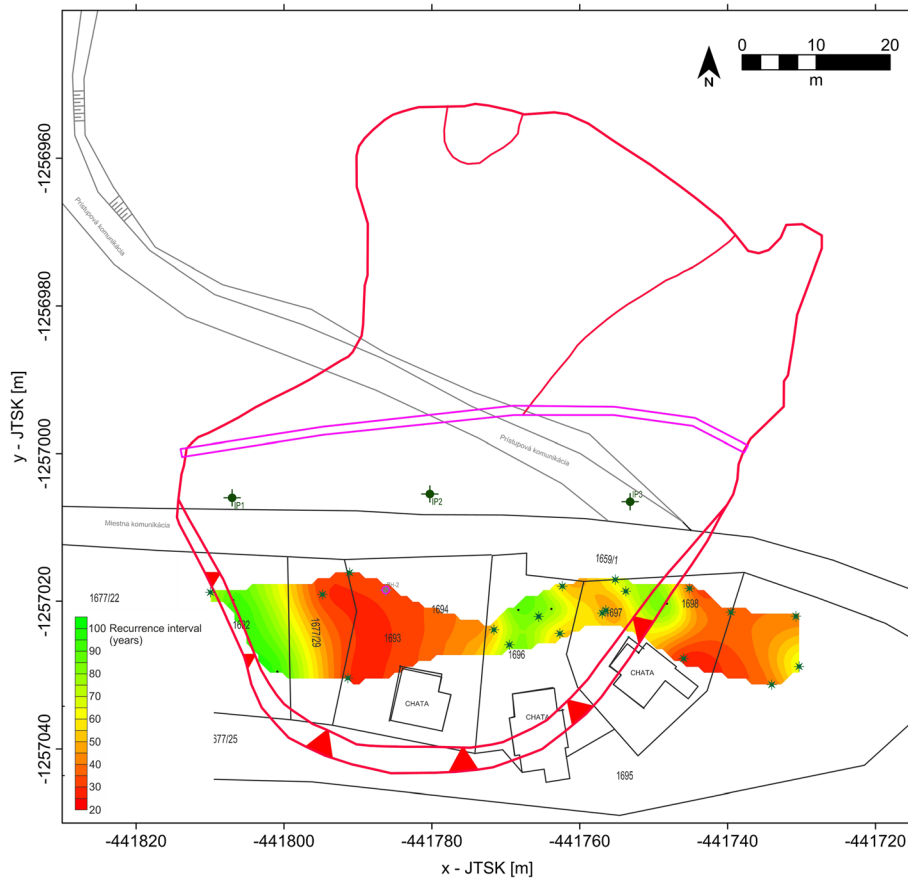


Fig. 9 The spatial distribution of recurrence intervals of landslide events on the area of young landslide

The input parameters of shear strength were based on the results of shear tests.

Results and discussion

Interpretation of geophysical measurements/survey

Profile ERT-H1

The inverse model (Fig. 7a) shows the landslide material making up the active part of the slope deformation as a heterogeneous body with a wide range of resistivity values (10–500 Ω/m). This range of values is caused by the landslide process itself, in which the integrity of the rock environment is disrupted and it separates into smaller blocks (higher resistivity) separated by a system of cracks filled with infiltrated water (lower resistivity). The shear plane of the active landslide (black line in the cross-section) appears as a sharp fall in resistivity between the landslide material and the underlying clay sediments from the fossil landslide, which have very low resistivity values (1–40 Ω/m). The ERT measurements were able to capture only partially the fossil shear surface found at a depth of 18–19 m in borehole BH-1, as shown by the broken line in the lower part of the inverse cross-section.

Profile ERT-H2

The active body of the landslide can be identified between metres 36 and 97 of the inverse cross-section (Fig. 7b), which corresponds

to observations on the surface. The active part of the landslide appears as an environment with high values of resistivity separated from the fossil slope deformation by zones of higher conductivity. The conductive zones can be interpreted as an active shear surface (black line), which corresponds to the active shear plane detected in borehole BH-1 at a depth of 5.6 to 5.9 m. The resistivity interface in the bottom part of the cross-section (broken line), which intersects with the fault zone detected at a depth of 18 to 19 m in the borehole, is interpreted as the fossil shear zone.

Interpretation of dendrochronological survey

In total, 39 trees (*Picea abies* (L.) Karst.) were sampled within the area of actual active landslide and on the connecting upslope area (old Pleistocene in age landslide). Together, 124 increment cores (tree ring series) were analysed. The mean age of all trees was 77.9 years (stdev 7.0 years). The oldest trees contained 89 tree rings in the sampling height, whereas the youngest only 62 tree rings. Fifty-nine growth disturbances were identified and dated from all trees (Table 2). Growth responses in the form of reaction wood slightly dominated (52.5%) over the abrupt growth suppressions (47.5%). The number of GD dominated on the area of young landslide (71.2%) in comparison with the old landslide (28.8%). In total, ten past landslide events were reconstructed using I_t index threshold. Seven landslide reactivations were reconstructed on the area of young landslide (1954, 1956, 1957, 1972, 1977, 1980 and 1990). The area of old landslide expressed only three reactivation years (1975, 2000 and 2016). Thus, the frequency of

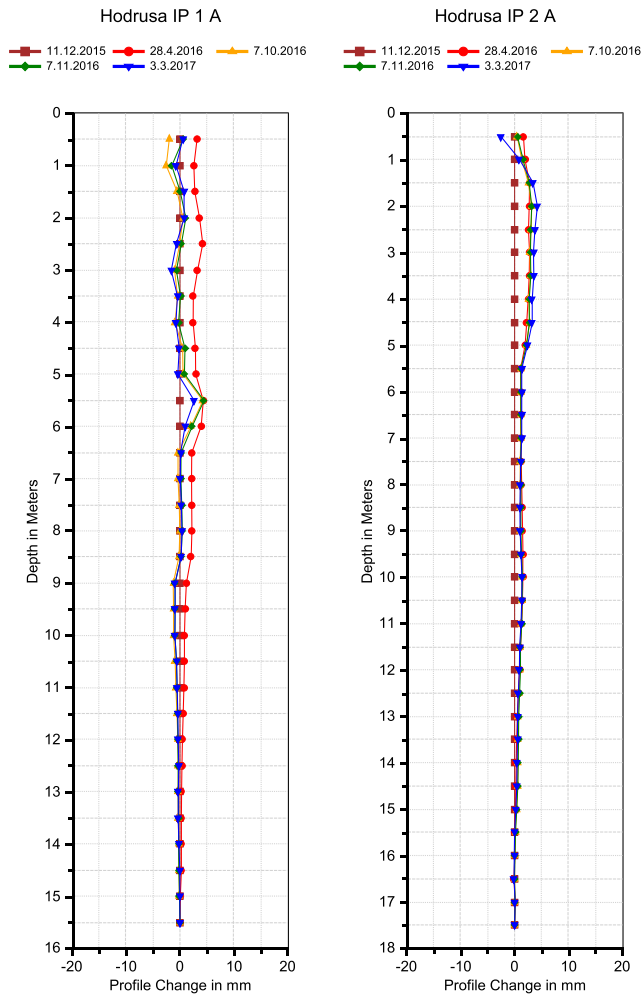


Fig. 10 Results of inclinometric measurements in boreholes IP1 (left) and IP2 (right)

landslide reactivations was higher in the area of young landslide (mean decadal frequency = 0.9 events/decade; Table 3). Events on the young landslide area reached higher I_t values (16.7%) in comparison the old landslide area (12.5%) in general (Fig. 8). The lowest reconstructed recurrence intervals (the highest events frequency) from individual trees were less than 20 years. The zones with such activity were reconstructed along both sides of the young landslide area (Fig. 9).

The relatively balanced numbers of two types of identified and dated growth disturbances (Table 2) suggest a different effect of past landslide movements to trees. Movements with dominated surface deformation effects induce the occurrence of reaction wood in the ring series of tilted trees (Lopez-Saez et al. 2012; Šilhán 2012). On the other hand, a comparable number of identified abrupt growth suppressions indicate subsurface movements that induced damage of tree root system (Šilhán et al. 2016). These results clearly correspond with inclinometric measurements that indicate both surface and subsurface landslide movements. Although, dendrogeomorphic techniques provide just minimal frequency of events, the temporal frequency of dated landslide movements is rather low in comparison with the activity of dated landslides in the wider area (Prokešová et al. 2010). This finding corresponds with generally infrequent and low magnitude of visible external growth

disturbances on trees. Moreover, the hypothesised lower activity of old landslide in comparison with the actual active one was verified. Both landslides probably behave partly independently as individuals and react to possible triggers in different way. Thus, the differences in event chronologies exist. For example, the dated event in 1975 (old landslide) can be associated with known falling of water level in the reservoir during winter months combined with heavy precipitation in March and April. On the other hand, the highest I_t of past landslide reactivation event was identified in 1977 (actual active landslide). This year is well known as a one of the most significant landslide years in the central Slovakia (Prokešová et al. 2010, 2013). An extended period of rainfall and snowmelt has been recognised as the main trigger of landslides in this year (Nemček 1982).

Analyses of inclinometric measurements

Inclinometric measurements were performed concurrently in boreholes IP1, whose depth was 15.0 m, and IP2, whose depth was 17.0 m (Fig. 10). In each borehole, an inclinometer casing with a diameter of 67 mm was installed up to the full height and held in place by a bentonite-cement mortar. The grooves were oriented in the direction of the expected movement. The zero and first inclinometer readings were taken on 11 December 2015 with follow-up on 28 April 2016, 7 October 2016, 7 November 2016 and finally on 3 March 2017 making a total of five readings including the zero reading. As the dates indicate, monitoring covered a period of 15 months. The inclinometer measurements were made using a Geokon inclinometer probe of American manufacture with a measurement interval of 0.5 m. After the completion of in situ measurements, the results were transferred electronically to a computer and evaluated in the program DigiPro2 from the American firm DGS (Durham Geo Slope Indicator). The movements captured by the inclinometer probe are shown using the “profile change”.

The zero measurement at inclinometer borehole IP1 was taken on 11 December 2015 and a further four-stage measurements were taken over a 15-month period. Figure 10-left shows that the borehole does not exhibit any more pronounced movement. The most noticeable movements were registered at a depth of 1.0 m–10.0 mm and a depth of 5.5 m–5.0 mm with the direction of movement towards the east, as can be seen in Fig. 10-right. This section of the landslide can be considered stabilised.

The zero measurement at inclinometer borehole IP2 was taken on 11 December 2015 and a further four-stage measurements were taken over a 15-month period. Figure 10 shows that the borehole does not exhibit any more pronounced movement. The most noticeable movements were registered at a depth of 0.5 m–7.8 mm and a depth of 2 m–5.0 mm with the direction of movement towards the east, as can be seen in Fig. 10. This section of the landslide can be considered stabilised. Standard results for inclinometric measurements include the size of movement and its azimuth (angle from north). The inclinometric boreholes IP1 and IP2 are built in such a way that the expected direction of movement and direction A are both approximately northwards (deviation $\pm 10^\circ$). The recorded direction of movement is actually perpendicular to this direction, i.e. direction B, west–east. Given this circumstance and given that the measured movements are very small, almost negligible, we have decided not to specify the exact azimuth of the recorded movements.

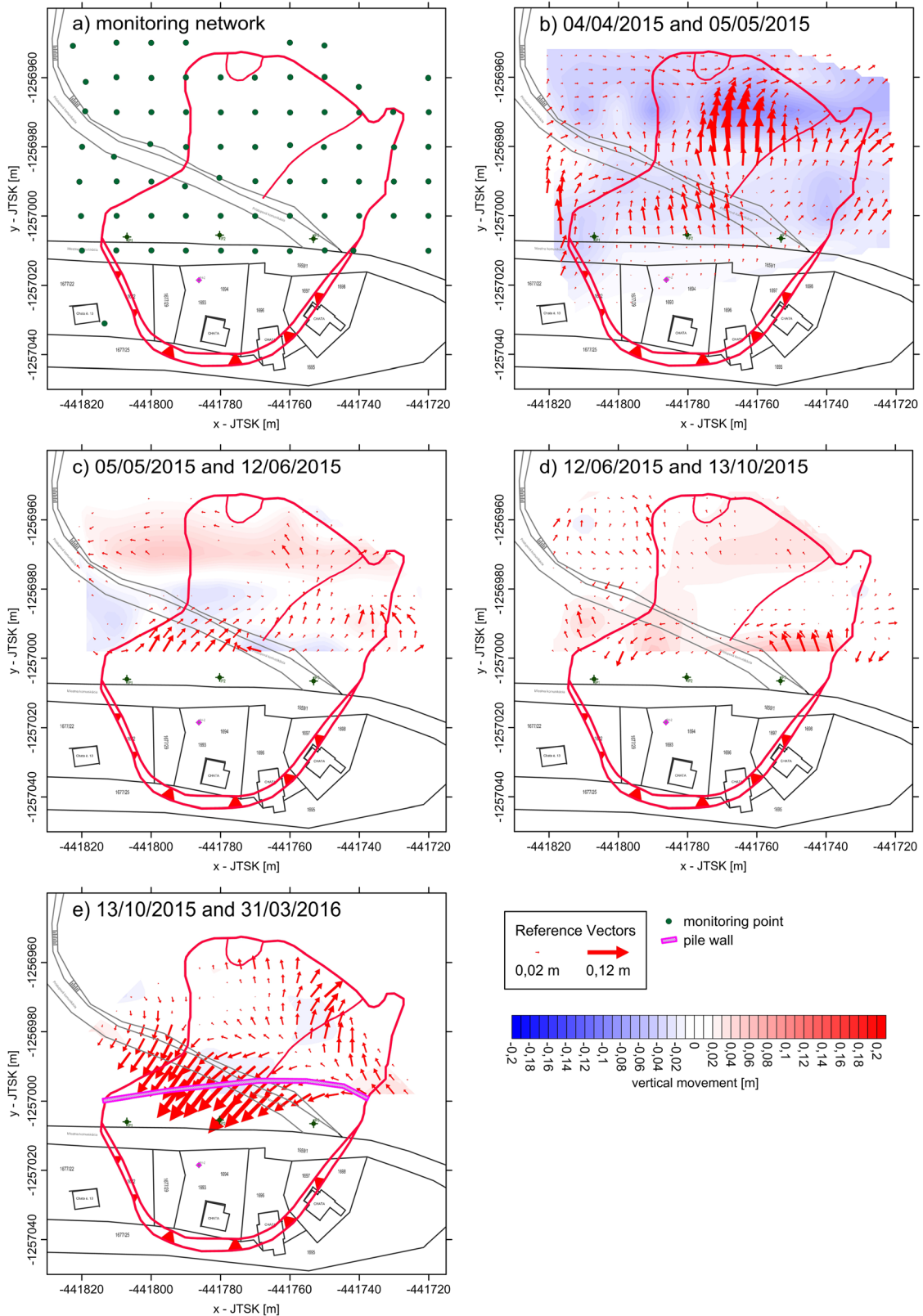


Fig. 11 Movement vectors of geodetic network points. **a** Measurement network. **b** Course of horizontal and vertical movements before construction of the pile wall. Horizontal movement to the north and subsidence of the whole area (emptying of the mining water reservoir). **c** Course of horizontal and vertical movements during construction of the pile wall, the wall was built from east to west. Uplift of the toe and right side of the landslide (by the landslide process). **d** The pile wall is finished but not anchored and the wall and its surrounding area are being rotated anticlockwise. **e** Backwards horizontal movement (to the southwest) in the vicinity of the pile wall and the area on the left flank of the landslide (could be caused by the anchoring of the wall to the slope or the refilling of the reservoir). Minimal vertical movements



Fig. 12 Deformation of target PG-2, 3 March 2017

Evaluation of movement vectors based on geodetic monitoring

After the first dates for comprehensive monitoring of the entire network of installed geodetic points, unexpected problems were encountered with points above the national road in the separation part of the landslide. Several points were interfered with; some were stolen, and the gradual growth of vegetation also made several points unusable. Later stages of monitoring concentrated only on the points in the reservoir area, on the national road and on the bank.

Each point was measured with an accuracy of $2 \text{ mm} + 0.5 \text{ ppm H}$ and $5 \text{ mm} + 0.5 \text{ ppm V}$, averaging 10 measurements on a bipod stand, with the standard deviations of the 10 measurements not exceeding 0.002 m in all directions, the defined accuracy of the GNSS rover technology used.

Monitoring took place at irregular intervals depending on the weather to enable all measurement campaigns to be conducted under relatively uniform conditions. The factors considered were weather stability, relative windlessness, the same amount of time passed since the last rainy days (saturation of the substrate with rainwater), an adequate interval since the previous measurement campaign. Measurements were conducted gradually at the following dates: 4 April 2015, 27 April 2015, 5 May 2015, 12 June 2015, 13 October 2015 and 31 March 2016. Figure 11a–e shows the changes in movement vectors of the points in the geodetic network chronologically linked to the course of the remediation measures (Kasza 2016).

After the building work on the pile wall prevented further movement of the displaced slope into the reservoir and the gradual flooding of the lowest monitoring points, the number of observed and measured points was reduced.

In order to ensure the comparability and relevance of measurements, several measurements were repeated during each campaign (on average 5–7% of the measurements per campaign) and reference measurements were taken using the geodetic points set up by the employees of Slovak Water Management Enterprise, state enterprise, Banská Bystrica. These points were situated on the dam body, on the water- and air-side slopes and on the discharge structure. At least 10 such reference points were measured on each occasion.

After the last measurement day (5 April 2016), a file of all the data collected in every measurement campaign was put together in Microsoft Excel. The resulting table was used to create a map for interpretation in the Surfer 11 program. Maps of the vertical subsidence and horizontal movements registered over time at individual points in different intervals were generated using the Kriging interpolation method.

Horizontal movement and its direction are represented by arrows, the length and size of the arrow reflect the magnitude of movement and the arrow's orientation shows its direction. Vertical movement is shown in the form of a contour map (blue—subsidence, red—uplift). The map header shows two different measurement dates selected for mutual comparison.

Horizontal movements of measured geodetic network points for individual time periods between measurement dates correspond substantially to expectations. However, the direction of movement and its dynamics are partly influenced by the course of the construction and technical works on the discharge object. An example is the construction and compaction of the access road from the main state road to the water reservoir during the months of May to June 2015 with a change in the direction of movement of the points above this road (Fig. 11d). However, these factors can not overlap the evident shift of most points in the downward direction, what ultimately contribute to a definitive decision to stabilise slope by remediation works. Figure 11d, e illustrates a change in the direction of displacement by about 180° . The backward shift is apparently due to the definitive anchoring of the pilot wall and changes in tensile stresses.

Evaluation of gypsum targets

Another easy method that was used to observe slope movements and the effectiveness of remedial works was evaluation of deformation on gypsum targets. On 30 October 2015, we installed nine gypsum targets on three chalets that had been significantly damaged by the landslide and which were situated in the main scarp area of the landslide.

The first deformation affected target PG-1 between April and October 2016, which was 10 months after completion of the remedial works. Between December 2016 and March 2017, the first

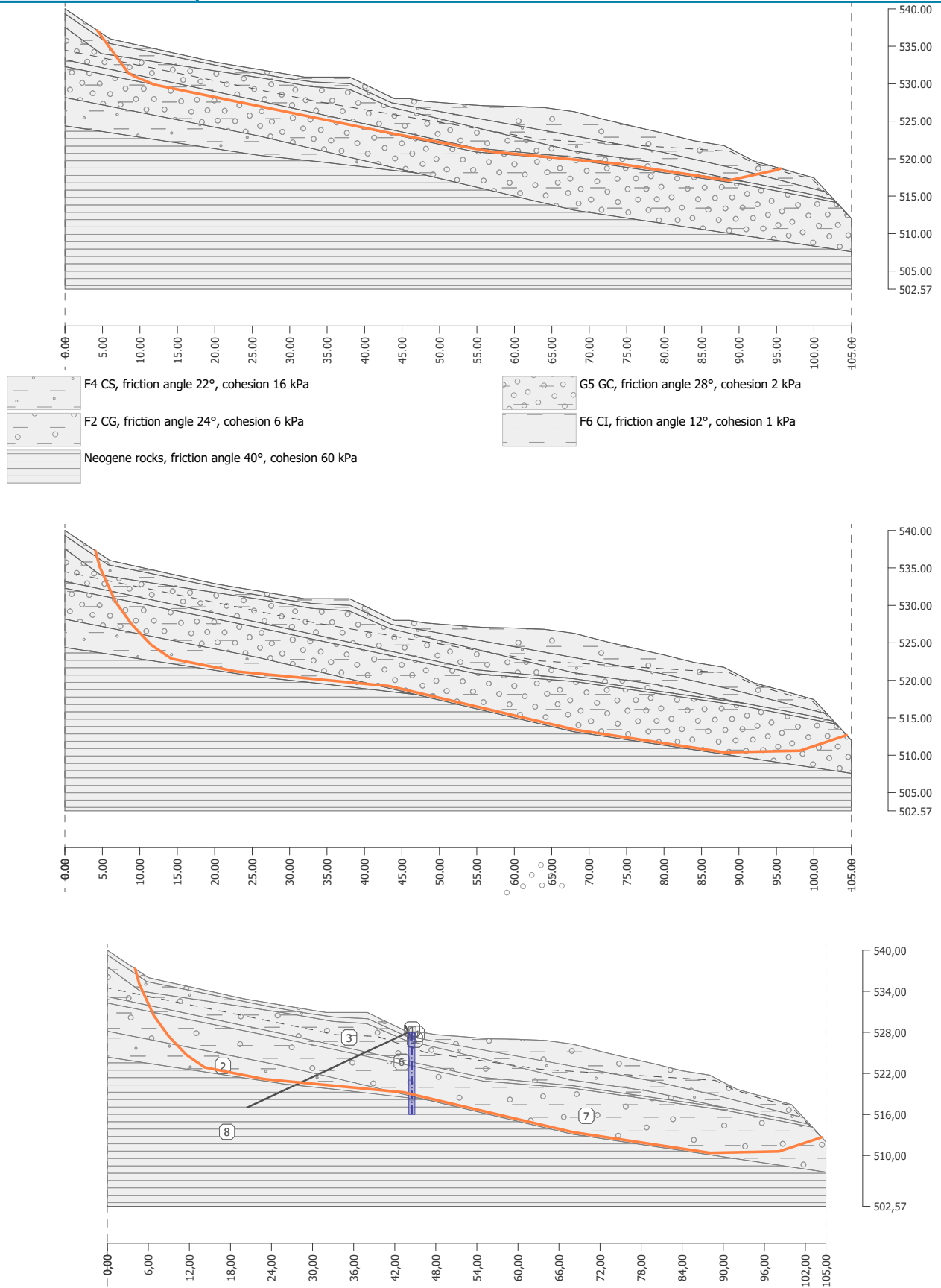


Fig. 13 Stability calculations. a Verified shear plane. b Basal shear plane. c Stability calculation with remediation elements

Table 4 Results of stability calculations

Profile	Soils and properties	ϕ [°]	c [kPa]	γ [kN/m ³]	Shear plane	Method of calculation	Fs—before remediation works—groundwater level 3.9 m under terrain	Fs—before remediation works—groundwater level 2.6 m under terrain	Fs—after remediation works—groundwater level 2.6 m under terrain
	F4 CS	22	16	18.5	Verified	Sarma	1.16	1	5.49
	F2 CG	24	6	19.5					
	G5 GC	28	2	19.5					
	F6 CI	12	1	19.5	Basal	Sarma	1.71	1.69	2.32
	Neogene	40	60	25					

deformation was observed on target PG-2 at the same chalet. The other targets remained without deformation throughout observation. After May 2016, it was no longer possible to monitor deformation of targets G-1 to G-5 because they were removed when the chalet was reconstructed during the summer. Figure 12 shows the deformation of target PG-2 in March 2017, which is nearly identical with the deformation in December 2016. The deformations are very small, not exceeding 1–2 mm. It is evident that movement on such a small scale cannot be attributed to active slope deformation. It may have been caused by the subsequent consolidation of the slope deformation. Compared with the deformations that occurred before remediation of the landslide, these are negligible.

Evaluation of stability conditions and remediation works

The input data for the evaluation comes from long-term measurements of the groundwater level, the geotechnical parameters of the soils identified before and during the implementation of stabilisation work and the parameters of the stabilisation structures. When calculating stability, the groundwater level entered for the first modelled state is that identified at the time of implementation of the engineering geological survey, and the groundwater level entered for the second state reflects conditions after the installation of remediation elements and is based on the results of systematic observations.

Stability evaluation was based on the identified shear plane (Fig. 13a) and the basal shear zone (Fig. 13b). Within the profile, also several hypothetical critical shear planes were calculated. The shear plane was given as both rotational and translational. The calculations for translational shear plane used Sarma's method and those for rotational ones used Bishop's method.

At the present groundwater level, the stability level is 1.16. If the groundwater level is raised by 1.3 m, the stability level is 1. The stability level of the basal shear surface is 1.71, which means that the probability of this shear surface's reactivation is low.

In the next step, in the stability assessment, factor of safety (Fs) was calculated for detected and basal shear plane, including the effect of the remedial works (Fig. 13c), the factor of safety for the detected shear surface based on Sarma's method is 5.49 and the factor of safety for the basal shear surface based on Sarma's method is 2.32 (Table 4).

Conventional threshold of Fs for permanent constructions has a value of 1.5, which presents satisfactory safety level. For special constructions, like this one is, the value of Fs is set by structural engineer also taking into account other plans with future land use. In our case, the road will be enlarged in near future, so also dynamical loads will increase.

The remediation of the landslide (Fig. 14) using an anchored pile wall was carried out in accordance with the design documentation between 21 October and 30 November 2015. To facilitate the construction of the anchored pile wall and make it easier for heavy plant to access the site, a work platform reinforced with a layer of aggregate was built before work commenced. The wall consists of 52 reinforced concrete piles 12.0 m in length, 900 mm in diameter, with a total length of 624 m. The piles were drilled by a SOILMEC drill rig. The concrete used for the piles is grade C25/30 reinforced with B500b concrete steel basket. The heads of the piles were fastened by anchoring reinforced concrete beams with dimensions 800 × 1100 mm and a length of 78.0 m. The concrete



Fig. 14 a View of the anchored reinforced concrete wall. b Aerial view of remedial works in progress. c Drilling the piles

in the beam is grade C25/30 with B500B concrete steel. The pile wall is further secured by 26 cable anchors at intervals of 3.0 m. The anchors are mounted to the beam through a steel pipe with a diameter of 219/7 mm ending with a 300 × 300-mm steel plate. The length of the anchors is 26 m with a root length of 10 m. The total length of the anchors is 676.0 m. The tilt of the anchors from the horizontal is 25°. The anchors are preloaded with a force $P_k = 300$ kN, which represents 50% of the maximum characteristic force when fully burdened by a landslide in its definitive stage $P_k = 600$ kN (Gomolčák 2015).

Conclusion

This manuscript deals with a multidisciplinary approach to the assessment of landslide area at the Lower Hodruša mining water reservoir, which belongs to the UNESCO cultural heritage.

Analysis of the geodetic monitoring results from the network of temporarily stabilised points permitted the quantification of vertical and horizontal changes in individual parts of the collapsed slope and its dynamics during construction work in the reservoir area. This was of key importance for understanding the development of slope deformation over time and its relationship to climatic factors, the hydrological situation, the properties of the rock mass and the ongoing construction work.

All epochs of landslide reactivation or increases in the size of cracks in the slope above the reservoir can almost certainly always be dated to the week following at least three previous weeks with a

total precipitation greater than 30 mm/week. Another case is reactivation caused by a single week with aggregate rainfall exceeding 60 mm/week. As an analysis of precipitation data showed, the events of 2013 were a combination of both conditions. Similar conditions were also recorded in the years 1975 and 1977.

It is likely that another necessary fundamental condition was the reduction of the water level in the reservoir, which reduced and eliminated the stabilising effects of the hydrostatic pressure of the water column on the slope and a corresponding increase in pore pressure that encouraged the gravitational descent of the landslide through differences in water saturation in the exposed rock in the reservoir area.

Dendrogeomorphic (tree ring based) analysis enabled to identify several minor landslide reactivations preceding the 2014 event. This means that the landslide area was active even in the past, but these events were not detected, probably because of the low magnitude of movements. The most significant pre-2014 event was dated to 1977, when several landslides were activated in the wider area. It means that the studied landslide reacts to hydrometeorological triggers as well. Moreover, the character of identified growth disturbances in the tree ring series corresponds to the findings from the inclinometric measurements.

Ongoing evaluation of vertical and lateral displacements and stability calculations was one of the determining factors in the decision to seek a means for fixing the collapsed slope by means of civil engineering works. Analysis of the obtained results supports

the decision of the administrator, Slovak Water Management Enterprise, state enterprise, Banská Bystrica, to build a pile wall in front of the landslide. The slope needs to be fixed in this way whenever there is a reduction in the level of the reservoir (for whatever reason), and it is not possible to guarantee or expect long-term climatic conditions favourable for slope stability.

The set of technical works (drilling, sampling, laboratory testing, gypsum targets observation), geophysical measurements (ERT), dendrochronology, geodetic monitoring, inclinometric measurements, as well as stability calculations was used as qualitative landslide hazard assessment in relation to water reservoir. The results of the measurements and their continuous interpretation described in the manuscript led to the decision-making process with regard to the remediation works design. Under usual conditions, only part of these measurements, respectively technical works, are realised in a frame of engineering geological investigation in landslide prone areas. Thanks to the fact that Lower Hodruša mining water reservoir belongs to the UNESCO cultural heritage, we were able to design and implement this wider and more time-consuming survey.

Funding information This work was partially supported by the Slovak Research and Development Agency under contracts no. APVV-0129-12, APVV-16-0146 and by the Scientific Grant Agency of the Ministry of Education, Science, Research and Sport of the Slovak Republic and the Slovak Academy of Sciences (VEGA) within the project no. 1/0559/17 and the Operational Programme Research and Development funded by the ERDF grant no. ITMS-26210120024, Restoration and building of infrastructure for ecological and environmental research at the Matej Bel University of Banská Bystrica.

References

- Alestalo J (1971) Dendrochronological interpretation of geomorphic processes. *Fennia* 105:1–139
- Auken E, Pellerin L, Christensen NB, Sørensen K (2006) A survey of current trends in near-surface electrical and electromagnetic methods. *Geophysics* 71(5):G249–G260
- Ceylan A, Karabork H, Ekozoglu I (2011) An analysis of bathymetric changes in Altınapa reservoir. *Carpathian J Earth Environ Sci* 6(2):15–24
- Corona C, Lopez Saez J, Stoffel M (2014) Defining optimal sample size, sampling design and thresholds for dendrogeomorphic landslide sampling. *Quat Geochronol* 22:72–84
- Čech V, Krokusová J (2017) Utilisation of environmentally degraded area by mining activity: a case study of Slovinky tailing impoundment in Slovakia. *Acta Montanistica Slovaca* 22(2):180–192
- Dahlin T, Zhou B (2004) A numerical comparison of 2D resistivity imaging with 10 electrode arrays. *Geophys Prospect* 52(5):379–398
- Dahlin T (2001) The development of DC resistivity imaging techniques. *Comput Geosci* 27(9):1019–1029
- Floris M, Bozzano F (2008) Evaluation of landslide reactivation: a modified rainfall threshold model based on historical records of rainfall and landslides. *Geomorphology* 94:40–57
- Fuska J, Kubinský D, Weis K, Lackóová L, Pokrývková L, Leitmanová M, Panagopoulos T (2017) Area-storage capacity curve of historic artificial water reservoir Ottergrund, Slovakia—assessment of the historical data with the use of GIS. *J Ecol Eng Warszawa Polish Soc Ecol Eng (PTIE)* 18(1):49–57
- Gomolčák M (2015) Remedial works on active landslide Hodruša Hámre. Final report. GEOKONTAKT Ltd., Košice
- Griffiths DH, Barker RD (1993) Two-dimensional resistivity imaging and modelling in areas of complex geology. *J Appl Geophys* 29(3):211–226
- Choiński A, Ptak M (2009) Lake infill as the main factor leading to lake's disappearance. *Pol J Environ Stud* 18(3):347–352
- Janský B, Schulte A, Česák J, Rios Escobar V (2010) The Mladotice Lake, western Czechia: the unique genesis and evolution of the lake basin. *Geografie Praha Czech Geogr Soc* 115(3):247–265

- Kašiarová E (2003) Lower Hodruša water reservoir, Štiavnické bane. Newsletter BEVEX-Mining research Prievidza, vol. 2–4
- Kasza R (2016) Monitoring of the reactivated surface landslide in the area of Dolné Hodrušské Lake. Bachelors thesis, Matej Bel University, Faculty of Natural Sciences, Department of Geography and Geology, 48 p
- Konečný V, Lexa J, Halouzka R, Hók J, Vozár J, Dublan L, Nagy A, Šimon L, Havrila M, Stolar M, Polák M, Vozár J, Pristaš J (1998) Geological map of Štiavnické vrchy Mts. and Pohronský Inovec at a scale 1:50 000. GSSR, Bratislava
- Kubinský D, Lehotský M, Weis K (2014a) Changes in bathymetry and land cover of riparian zone of an old artificial water reservoir Veľký Kolpašský. *Carpathian J Earth Environ Sci* 9(1):171–178
- Kubinský D, Weis K, Fuska J, Lehotský M, Petrovič F (2014b) Changes in retention characteristics of 9 historical artificial water reservoirs near Banská Štiavnica, Slovakia. *Open Geosciences: De Gruyter Open Ltd* 7(1):880–887
- Ministry of Environment of the Slovak Republic (ed) (2002) Landscape atlas of the Slovak Republic, 1st edn. Slovak Environmental Agency, Banská Bystrica 344 p
- Lexa J (2016) Specialized geological map of Rozália Mine (Hodruša-Hámre), M1: 5000
- Loke MH, Acworth I, Dahlin T (2003) A comparison of smooth and blocky inversion methods in 2D electrical imaging surveys. *Explor Geophys* 34(3):182–187
- Lopez-Saez J, Corona C, Stoffel M, Astrade L, Berger F, Malet JP (2012) Dendrogeomorphic reconstruction of past landslide reactivation with seasonal precision: Bois Noir landslide, southern French Alps. *Landslides* 9:189–203
- Migoń P, Kacprzak A, Malik I, Kasprzak M, Owczarek P, Wistuba M, Pánek T (2014) Geomorphological, pedological and dendrochronological signatures of a relict landslide terrain, Mt Garbatka (Kamienne Mts), SW Poland. *Geomorphology* 219:213–231
- Nemček A (1982) Landslides in Slovak Carpathians. Veda, Bratislava, p 319 (In Slovak)
- Pánek T, Šilhán K, Tábořík P, Hradecký J, Smolková V, Lenárt J, Brázdil R, Kašičková L, Pazdur A (2011) Catastrophic slope failure and its precedings: case of the May 2010 Girová Mountain long-runout rockslide (Czech Republic). *Geomorphology* 130:352–364
- Petley DN, Allison RJ (1997) The mechanics of deep-seated landslides. *Earth Surf Process Landf* 22:747–758
- Prokešová R, Kardoš M, Medved'ová A (2010) Landslide dynamics from high-resolution aerial photographs: a case study from the Western Carpathians, Slovakia. *Geomorphology* 115:90–101
- Prokešová R, Medved'ová A, Tábořík P, Snopková Z (2013) Towards hydrological triggering mechanisms of large deep-seated landslides. *Landslides* 10:239–254
- Shroder JF (1978) Dendrogeomorphological analysis of mass movement on Table Cliffs Plateau, Utah. *Quat Res* 9:168–185
- Smolková V, Pánek T, Hradecký J (2009) Holocene sedimentation dynamics and average catchment denudation acquired from the sedimentary basins of the landslide-dammed lakes in the Flysch Carpathians. In: *Geomorfologicky sbornik 8: Sbornik abstraktů. Zapadočeska univerzita v Plzni, Ustav struktury a mechaniky hornin AV ČR, v. v. i., Česka asociace geomorfologů*, p 52
- Stoffel M, Bollschweiler M (2008) Tree-ring analysis in natural hazards research—an overview. *Nat Hazards Earth Syst Sci* 8:187–202
- Stoffel M, Butler DR, Corona C (2013) Mass movements and tree rings: a guide to dendrogeomorphic field sampling and dating. *Geomorphology* 200:106–120
- Šilhán K (2012) Dendrogeomorphological analysis of the evolution of slope processes on flysch rocks (Vsetínské vrchy Mts; Czech Republic). *Carpathian J Earth Environ Sci* 7:39–49
- Šilhán K (2017) Evaluation of growth disturbances of *Picea abies* (L.) Karst. to disturbances caused by landslide movements. *Geomorphology* 276:51–58
- Šilhán K, Prokešová R, Medved'ová A, Tichavský R (2016) The effectiveness of dendrogeomorphic methods for reconstruction of past spatio-temporal landslide behaviour. *Catena* 147:325–333
- VIAS (2005) Vienna Institute of Archaeological Science: Time Table, Installation and instruction manual. Ver. 2.1, Vienna
- Vonšáková D (2017) Virtual reconstruction of the extinct historic water reservoir and the possibility of its use in geotourism, Master thesis, University of Matej Bel in Banská Bystrica. Faculty of Natural Sciences, Department of Geography and Geology, 74 p
- Weis K, Kubinský D (2014) Analysis of changes in the volume of water in the Halčianske reservoir caused by erosion as a basis for watershed management. *Geografie Praha, Czech Geogr Soc* 119(2):126–144

M. Bednarik (✉) · R. Tornyai · F. Holzer

Faculty of Natural Sciences, Department of Engineering Geology, Comenius University in Bratislava, Bratislava, Slovak Republic
Email: mbednarik@uniba.sk

R. Putiška · I. Dostál

Faculty of Natural Sciences, Department of Geophysics and Environmental Geology,
Comenius University in Bratislava,
Bratislava, Slovak Republic

K. Šilhán

Faculty of Natural Sciences, Department of Physical Geography and Geoecology,
University of Ostrava,
Ostrava, Czech Republic

K. Weis

Banská Bystrica, Faculty of Natural Sciences, Department of Geography and Geology,
Matej Bel University,
Banská Bystrica, Slovak Republic

I. Ružek

Faculty of Natural Sciences, Department of Physical Geography and Geoecology,
Comenius University in Bratislava,
Bratislava, Slovak Republic